BMC Cardiovascular Disorders

RESEARCH

Open Access

Single-cell transcriptomics reveals writers of RNA modification-mediated immune microenvironment and cardiac resident Macro-MYL2 macrophages in heart failure

Yao-Lin Yang[1], Xiao-Wei Li[1], Hai-Bin Chen[1], Qi-Dong Tang[1], Yu-Hui Li[1], Ji-Ying Xu[1] and Jia-Jia Xie[1*]

Abstract

Background Heart failure (HF), which is caused by cardiac overload and injury, is linked to significant mortality. Writers of RNA modification (WRMs) play a crucial role in the regulation of epigenetic processes involved in immune response and cardiovascular disease. However, the potential roles of these writers in the immunological milieu of HF remain unknown.

Methods We comprehensively characterized the expressions of 28 WRMs using datasets GSE145154 and GSE141910 to map the cardiac immunological microenvironment in HF patients. Based on the expression of WRMs, the immunological cells in the datasets were scored.

Results Single-cell transcriptomics analysis (GSE145154) revealed immunological dysregulation in HF as well as differential expression of WRMs in immunological cells from HF and non-HF (NHF) samples. WRM-scored immunological cells were positively correlated with the immunological response, and the high WRM score group exhibited elevated immunological cell infiltration. WRMs are involved in the differentiation of T cells and myeloid cells. WRM scores of T cell and myeloid cell subtypes were significantly reduced in the HF group compared to the NHF group. We identified a myogenesis-related resident macrophage population in the heart, Macro-MYL2, that was characterized by an increased expression of cardiomyocyte structural genes (*MYL2*, *TNNI3*, *TNNC1*, *TCAP*, and *TNNT2*) and was regulated by TRMT10C. Based on the WRM expression pattern, the transcriptomics data (GSE141910) identified two distinct clusters of HF samples, each with distinct functional enrichments and immunological characteristics.

Conclusion Our study demonstrated a significant relationship between the WRMs and immunological microenvironment in HF, as well as a novel resident macrophage population, Macro-MYL2, characterized by myogenesis. These results provide a novel perspective on the underlying mechanisms and therapeutic targets for HF. Further experiments are required to validate the regulation of WRMs and Macro-MYL2 macrophage subtype in the cardiac immunological milieu.

*Correspondence:
Jia-Jia Xie
xiejiajia1983@163.com

Full list of author information is available at the end of the article

Keywords Heart failure, Writers of RNA modification, Immune microenvironment, WRM score, Cardiac resident macrophages

Introduction

Heart failure (HF) is a syndromic outcome of abnormalities in cardiac structure, function, rhythm, or conduction [1]. It occurs when the heart is unable to effectively pump blood due to cardiac muscle weakness or stiffness [2, 3]. The most prevalent risk factors contributing to HF include genetics, diabetes, coronary artery disease, obesity, high blood pressure, and chronic kidney disease [4, 5]. HF affects about 13.7 million patients in China, and an estimated 3.0 million Chinese adults experience incident HF each year [6]. HF imposes a substantial burden in terms of morbidity, mortality, and health care expenses. The prevention and management of HF are challenging, and its prevalence may continue to rise in the foreseeable future. The prognosis of HF patients remains poor, despite the advancements that have been made in the medical treatment of HF, including the use of angiotensin converting enzyme inhibitors [7], angiotensin receptor-neprilysin inhibitors [8, 9], sodium/glucose cotransporter 2 (SGLT2) inhibitors [10, 11], spironolactone [12], inhibitors of soluble epoxide hydrolase [13], and inflammation modulators [14]. HF alters cardiac proteins and hormones [15–17], which is relevant to the diagnosis, therapy, and prognosis of HF patients. Therefore, it is imperative to improve the prognosis of HF patients and to provide them with effective therapy.

Cardiac injury is associated with a systemic immune response. The immune response is beneficial during the early stages of cardiac injury. After a distinct tissue injury, immune cells like neutrophils and monocytes are initially recruited to facilitate effective tissue repair [18]. Neutrophils exhibit distinct phenotypes and function that can promote both tissue repair and collateral damage processes [19]. Macrophages, which are generated by monocytes, are responsible for wound healing, eliminating apoptotic cells, fibroblast-to-myofibroblast differentiation, and the removal of debris in cardiac repair [20]. Regulatory T cells (Tregs) are also involved in cardiac injury, where they inhibit excessive inflammatory responses and promote scar formation [21]. In addition to the cells mentioned above, other immune cells such as B cells [22], T cells [18], natural killer (NK) cells [23], dendritic cells (DC) [24], and mast cells [25] have been shown to be involved in cardiac injury. The timely transition from pro-inflammatory to anti-inflammatory activities of the immune response is crucial during cardiac repair, and a dysregulated immune response leads to HF [18]. The expander and activation of immune cells have been identified through single-cell RNA sequencing (scRNA-seq) in the HF model [26]. This process induces fibrosis by recruiting monocyte-derived macrophages [27]. Therefore, examining immune microenvironment regulation is essential for understanding HF development.

RNA modification is widespread in nature. Readers, erasers, and writers are responsible for the binding, removal, and addition of the modified bases to influence cellular biological processes [28], which are performed by RNA modifications. More than 170 modifications in RNA levels have been identified, including but not limited to N6-methyladenosine (m6A), N1-methyladenosine (m1A), N7-methylguanosine (m7G), alternative polyadenylation (APA), and adenosine-to-inosine (A-I) [29]. In eukaryotes, the m6A modification is the most prevalent and abundant mRNA modification, occurring in most non-coding RNA [30]. The m1A modification is reversible, and tRNA is the most modified RNA [31]. m7G binds to the 5' cap co-transcriptionally during transcription initiation and exists internally within mRNA, tRNA, and rRNA [32]. APA cleaves mRNA to add poly A tails for generating transcripts that contain different lengths of 3'-untranslated region or coding regions [33]. A-I RNA modification, which converts adenosines to inosines by deamination in RNA, is widely found in pre-mRNA, mRNA, and non-coding RNA [34]. However, a comprehensive analysis of these RNA modification regulators in HF has not been reported.

Dysregulation of epigenetic modification and aberrant gene expression occur frequently in HF patients. In cardiovascular diseases, previous research has indicated that metabolic and regulatory pathways are primarily affected by alterations of m6A RNA methylation during progression to HF [35]. Cardiomyocyte hypertrophy stimulates methyltransferase-like 3 (METTL3)-mediated methylation of m6A, whereas the absence of METTL3 accelerates HF progression and drives eccentric cardiomyocyte remodeling and dysfunction [36]. METTL3 expression is consistently increased in the fibrotic cardiac tissue of mice, which contributes to collagen accumulation [37]. RNA modification regulators also modulate the immune response to influence HF development. For instance, the immunological microenvironment of HF [38] is highly associated with the m7G modification. RNA modification patterns mediated by differential m6A regulators determine the pattern of immunological cell infiltration in atrial fibrillation [39]. A high m6A modification pattern is associated with elevated cardiac infiltration of immune cells in patients with coronary heart disease [40]. Moreover, different m6A regulators exhibit unique associations with immune cells in ischemic cardiomyopathy

[41]. These investigations indicate that RNA modification is a vital factor in cardiac remodeling and immune response reprogramming. A comprehensive understanding of the regulatory network of various RNA modifications in the immune milieu of HF will help develop immunotherapeutic strategies.

In this study, we systematically examined the modification patterns of writer of RNA modification (WRM) in the immune microenvironment of HF using publicly available HF datasets. Additionally, we investigated the infiltration and functioning of specific immune cell subtypes regulated by WRMs. Importantly, we identified a myogenesis-associated population of cardiac resident macrophages (CRMs), termed Macro-MYL2, which expresses high levels of cardiomyocyte structural genes and is regulated by the m1A writer TRMT10C. Our results demonstrate a significant impact of WRMs on the immunological microenvironment in HF, suggesting a novel approach for treating HF.

Materials and methods

Datasets preprocessing

The scRNA-seq dataset GSE145154 [42] was derived from the Gene Expression Omnibus (GEO) database, containing 10 HF samples and 5 non-HF samples (NHF). These samples were isolated from the myocardium and the corresponding peripheral blood. The scRNA-seq data, quantified using Cell Ranger from 10× Genomics with default parameters, was analyzed using the Seurat package in the R software. We quantified the number of genes and unique molecular identifiers (UMIs) for each cell and retained only high-quality cells meeting the following criteria: 500–9,000 genes, 500–100,000 UMIs, less than 25% of mitochondrial gene counts, and less than 3% of erythrocytes. The DoubletFinder package was employed to identify doublets with default parameters. Principal component analysis and uniform manifold approximation and projection (UMAP) were utilized to conduct a comprehensive dimensionality reduction analysis on single-cell samples. The SingleR package and BlueprintEncodeData were investigated as reference data for auxiliary annotation. Subsequently, marker genes were identified for manual annotation of various clusters.

scRNA-seq data analysis

We utilized the R package "limma" to identify the differentially expressed genes (DEGs) for each cell cluster. Cell-cell communication and gene regulatory networks were constructed by CellChat and Single-Cell Regulatory Network Inference and Clustering (SCENIC) analysis, respectively. To identify marker genes for each cell cluster and DEGs between groups or cell types, the FindAllMarkers function in the Seurat package was employed, with the criteria of |log2 fold change| > 1 and p value < 0.05. Gene-set variation analysis (GSVA) was conducted for pathway enrichment analysis. Pseudotime trajectory analysis was performed using the Monocle2 package for. Gene Ontology (GO) and Kyoto Encyclopedia of Genes and Genomes (KEGG) enrichment analysis of DEGs was performed using R packages, including "topGO" (2.52.0), "clusterProfiler" (4.8.3), and "stringr" (1.5.0). The R package "Cibersort" (0.1.1) was utilized to analyze the proportion of infiltrated immune cells. We performed the correlation analysis using the R package ggcorrplot (0.1.4.1).

Identification of differentially expressed WRM

According to previous studies [29, 38], WRM-related genes were selected from m6A, m1A, APA, A-I, and m7G regulators. WRM scores for each cluster and cell type were calculated using single-sample gene-set enrichment analysis (ssGSEA) based on the expression levels of WRM-related genes. The statistical differences between groups were analyzed using the Wilcoxon test, and a p value < 0.05 was considered statistically significant.

Bulk RNA-seq data analysis

The R package "limma" (3.56.2) was used to normalize the bulk RNA-seq dataset GSE141910 [43], which was extracted from the GEO database. The dataset contained 200 HF samples and 166 NHF samples, and it was subsequently analyzed. The process of handling bulk RNA-seq data followed the scRNA-seq data analysis. Additionally, the R package "ggpubr" (0.6.0) was used to assess the expression of WRM-related genes in the HF and NHF samples in dataset GSE141910.

Consensus clustering analysis based on WRM

The R package "ConsensusClusterPlus" (1.64.0) was used for consensus clustering analysis according to the expressions of WRM-related genes in the 200 HF samples in the dataset GSE141910. Subsequently, differential and pathway enrichment analyses were conducted based on the consensus clustering results.

Isolation of cardiac macrophages

As demonstrated in prior research [27], cardiac macrophages were isolated from the ventricular myocardium of mice. Red blood cells were removed from the heart by flushing it with PBS. It was then minced into a slurry and digested in Hanks Balanced Salt Solution (21022CM, Corning) with 2.5 mM $CaCl_2$, 0.1% collagenase B (11088831001, Roche), 10 mM Hepes, and 2.4 U/ml Dispase II (04942078001, Roche) in a 37 °C water bath for 30 min. Immune cell-focused panels were utilized in flow cytometry to identify macrophages. The isolated macrophages were cultured in DMEM (10-013-CVRC, CORNING) supplemented with 10% fetal bovine serum

(10099141 C, GIBCO), 1× penicillin/streptomycin, 20 ng/ml of lipopolysaccharide (00497693, eBioscience), and 5% CO_2 at 37 °C.

Cell transfection

A total of 3×10^4 cells/mL of macrophages were seeded into 24-well plates. The *Trmt10c* overexpression plasmids were transfected into cardiac macrophages using lipo2000 (11668019, Thermo) at a final concentration of 50 nM.

RT-qPCR

Total RNA was extracted from macrophages employing the TRIzol LS reagent (10296028CN, Invitrogen, USA). RT-qPCR was performed using the following primers: *Trmt10c*-F: 5'-TGGGACAAATTGCTCTTAACAG C-3', *Trmt10c*-R: 5'-GTTGCTATGTTTAACCGTTTGG C-3', *Gapdh*-F: 5'-CAAAATGGTGAAGGTCGGTGT-3', *Gapdh*-R: 5'-GAGGTCAATGAAGGGGTCGTT-3'.

Western blot

The total proteins were isolated from macrophages and separated in a 10% SDS-PAGE gel. Subsequently, the proteins were transferred to a PVDF membrane (Millipore, USA). The proteins were incubated at 4 °C overnight with the primary antibodies anti-TRMT10C (1/2000, 29087-1-AP, Proteintech) and anti-GAPDH (1/15000, 60004-1-lg, Proteintech). Following this, the primary antibodies were incubated with the corresponding second antibodies goat anti-mouse IgG H&L (HRP, 1/1000, ab205719, Abcam) and goat anti-rabbit IgG H&L (HRP, 1/20000, ab6721, Abcam).

Immunofluorescence

The MLY2 protein in macrophages was identified using the primary antibody anti-MYL2 (10906-1-AP, Proteintech) after 48 h of cell transfection. The cells were fixed with methanol for 30 min, followed by sealing with 3% bovine serum albumin. The primary antibody was used to incubate cells at 4 °C overnight. The secondary antibody goat anti-rabbit IgG H&L (Alexa Fluor® 488, ab150077, Abcam) was then used to incubate cells at ambient temperature for 1 h in a dark room. The DAPI stain (C1006, Beyotime) was used to stain nuclei. An inverted fluorescence microscope was used to observe fluorescent images (NIKON). The Image Pro Plus software was used to measure the fluorescent intensity.

Statistical analysis

Student's t-test was used for comparisons between the two groups. $P<0.05$ values was set as indicating statistical significance.

Results

The scRNA-seq data reveals immune dysregulation in HF

The GSE145154 dataset was employed to examine the cellular milieu in failing hearts by analyzing $CD45^-$ cells in the myocardium and $CD45^+$ immune cells isolated from the myocardium and corresponding peripheral blood of 10 HF and 5 NHF samples [42]. After applying quality-control filtering, 72,041 quality-control-positive cells were obtained. This included 47,418 cells from HF samples and 24,623 cells from NHF samples (Fig. S1A). The unsupervised graph-based clustering revealed 10 major cell types, including endothelial cells, fibroblasts, smooth muscle cells (SMC), pericytes, cardiomyocytes, T cells, NK cells, B cells, myeloid cells, and mast cells (Fig. 1A and Fig. S1B). Compared with the NHF samples, we observed that the NK cells and T cells were augmented in the HF samples, whereas endothelial cells, fibroblasts, and myeloid cells were inhibited in HF progression (Fig. 1B). As shown in Fig. 1C, GSVA revealed an enrichment of the immune cells (T cells, NK cells, B cells, myeloid cells, and mast cells) in immune-associated pathways, such as IL-2/STAT5 signaling, IL-6/JAK2/STAT3 signaling pathway, inflammatory response, and interferon alpha/gamma response. The fibroblasts and endothelial cells were activated in epithelial mesenchymal transition, myogenesis, and angiogenesis that were related to cardiac remodeling. The cardiomyocytes were also enriched in oxidative phosphorylation and fatty acid metabolism, in addition to myogenesis. The cell-chat analysis revealed diverse interactions among these cell types (Fig. 1D), and the number of ligand-receptor pairs varied (Fig. S1C). In brief, these results comprehensively indicate the cell composition in the heart and reveal immune dysregulation in HF.

Landscape of WRMs in HF

To investigate whether the RNA modification impacted HF, we evaluated the expression of five major WRMs in the cardiomyocytes, including m6A writers (METTL3, METTL14, WTAP, RBM15, RBM15B, ZC3H13, KIAA1429), m1A writers (TRMT61A, TRMT10C, TRMT61B, TRMT6), APA writers (CPSF1, CPSF2, CPSF3, CPSF4, CSTF1, CSTF2, CSTF3, CFI, PCF11, CLP1, NUDT21, PABPN1), A-I writers (ADAR, ADARB1, ADARB2), and m7G writers (METTL1, WDR4) (Fig. 1E). The expression levels of WRMs were significantly different between the HF and NHF groups (Fig. S1D). The WRM scores of T cells, myeloid cells, endothelial cells, pericytes, fibroblasts, and SMC were significantly different between the two groups (Fig. 1F). Additionally, we observed that the WRMs were differentially expressed among these 10 cell types (Fig. 1G). Thus, WRM expression was abnormal in HF.

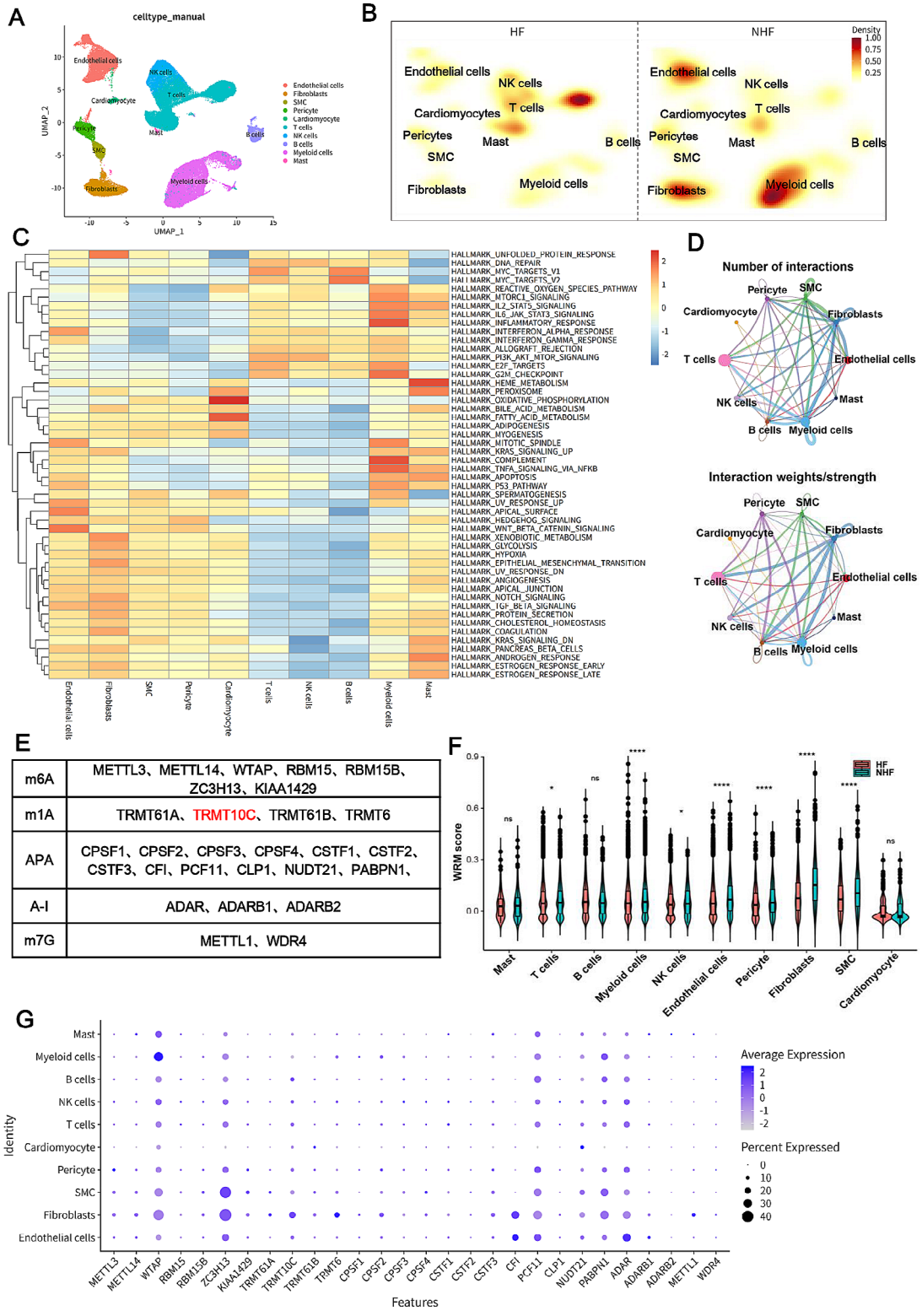

Fig. 1 Overview of WRMs in the scRNA-seq data for HF. (**A**) Cell type annotation by using the UMAP plot. (**B**) Cell density in the HF and NHF samples. The color changed from yellow to red, indicating low to high cell density. (**C**) HALLMARK pathway enrichment for 10 core cell types by GSVA analysis. (**D**) Number of interactions (top) and interaction weights/strength (bottom) among the main 10 cell types were determined using cell-chat analysis. The width was proportional to the number of ligand-receptor links. (**E**) Five major RNA modification writers. (**F**) WRM scores between HF and NHF patients. ns = not significant, *$p < 0.05$, **$p < 0.01$, and ***$p < 0.001$. (**G**) Expression profiles of WRMs in 10 cell types

WRM is related to the immune microenvironment in HF

We evaluated pairwise correlations between immune cells and pathway enrichment based on the WRM score. The findings revealed that WRM-scored immune cells were positively correlated with immune response (interferon gamma/alpha, IL6/JAK/STAT3 signaling, IL2/JAK/STAT5 signaling, complement, and inflammatory response), cell metabolism (glycolysis, fatty acid metabolism, adipogenesis, and cholesterol homeostasis), oxidative phosphorylation, cell development (apoptosis, PI3K/AKT/MTOR signaling pathway, p53 pathway, E2F targets, G2M check point, DNA repair, and mitotic spindle), and myogenesis (Fig. 2A). Given the heterogeneity and complexity of RNA modification, ssGSEA was performed to develop a WRM score model for four immune cell types based on WRM expression level to quantify the RNA modification pattern of each HF patient. The WRM-scored immune cells were divided into two groups: the WRM high group (score>0) and the WRM low group (score<0). We observed that the WRM high group experienced a higher infiltration of immune cells, including T cells, myeloid cells, NK cells, and B cells

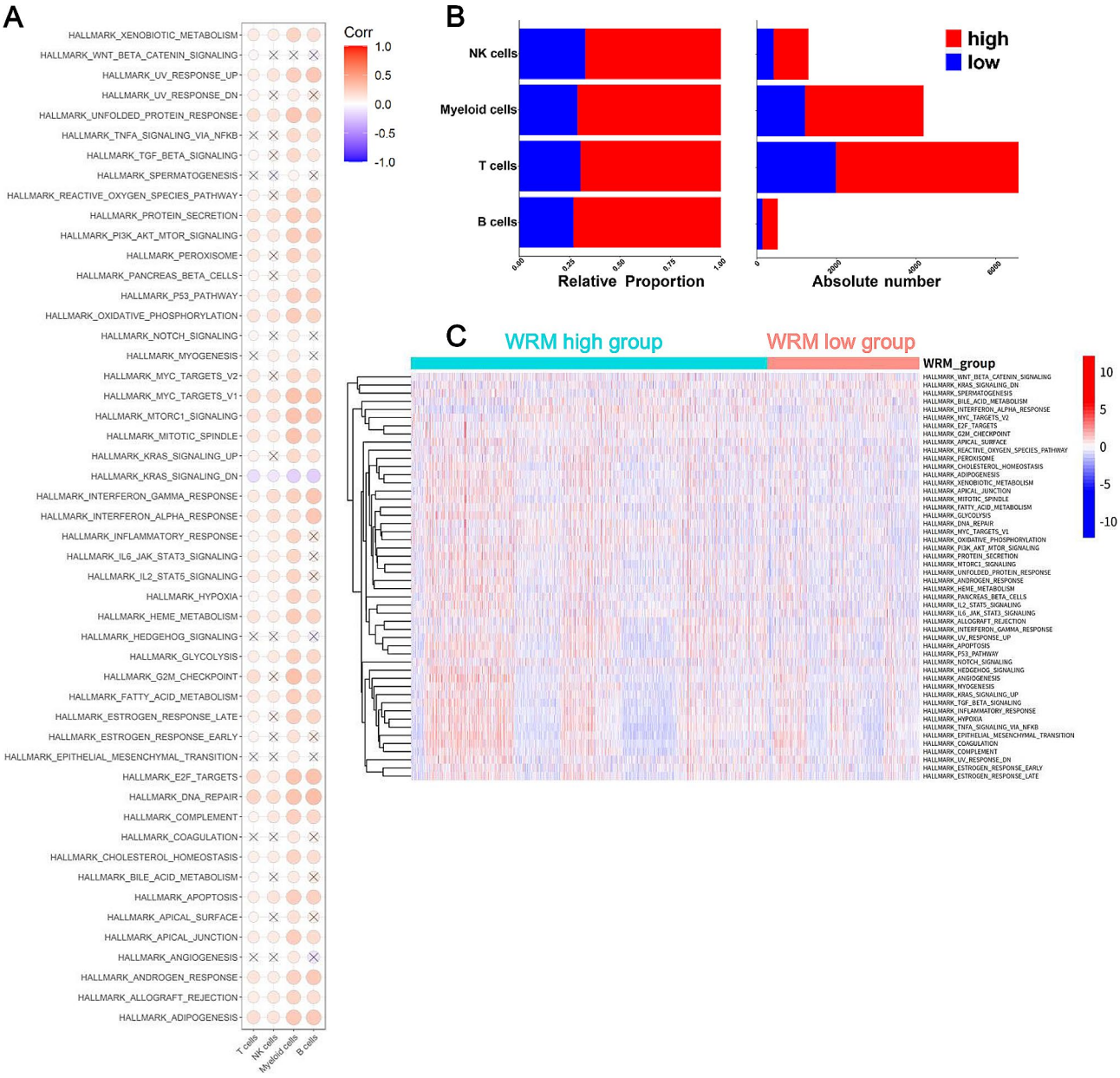

Fig. 2 WRM is involved in the regulation of the immune microenvironment in HF. (**A**) Bubble plot of HALLMARK pathway for WRM-scored immune cell types. (**B**) Bar diagram depicting the proportion and count of the four immune cell types in high- and low-WRM score group. (**C**) Heatmap visualizing the GSVA enrichment analysis revealed the activation states of HALLMARK pathways in the WRM high and WRM low groups

(Fig. 2B). The GSVA enrichment analysis was conducted to further characterize the functional enrichment of the two RNA modification patterns. The results indicated that the enrichment level of various pathways exhibited significant heterogeneity between the WRM low and the WRM high groups (Fig. 2C). Collectively, these results demonstrate that WRM is involved in the regulation of the immune microenvironment of the failing heart.

T cells in heart display heterogeneity and complexity and are associated with WRM

In HF patients, cardiac T cell infiltration has been documented, and various T cell subtypes have distinct functions in the heart [44]. To determine the potential roles of T cells in HF, they were re-clustered for further investigation. Based on the known marker genes and highly expressed genes, T cells were classified into 6 subtypes, including $CD4^+$ naïve T cells (Tn), $CD4^+$ tissue-resident memory (Trm) T cells, $CD8^+$ effector memory T (Tem) cells, $CD8^+$ effector memory cells re-expressing CD45RA (Temra), $CD8^+$ Tn cells, and γδT cells (Fig. 3A). The pseudotime analysis of T cell subtypes revealed that the terminals of the pseudotime trajectory were occupied by $CD8^+$ Tem cells, $CD8^+$ Temra cells, and γδT cells (Fig. 3B). Figure 3C illustrates the ratio of T cell subtypes in the HF and NHF groups. It was observed that the HF group exhibited a greater abundance of each T cell subtype than the NHF group. According to a growing body of evidence, macrophage migration inhibitory factor (MIF) can protect the heart following cardiac injury by activating the AMPK signaling pathway, inhibiting JNK pathway activation, and attenuating cardiomyocyte oxidative stress [45, 46]. The cell-chat analysis revealed the presence of a ligand-receptor complex (CD74-CD44) between cardiomyocytes and $CD8^+$ Tem cells via the MIF signaling pathway (Fig. 3D and Fig. S2A), implying that cardiomyocytes regulate T cells. To explore the functional difference in T cells between the HF and NHF groups, we conducted the DEG analysis (Fig. S2B). The GO enrichment analysis of the upregulated DEGs between the HF and NHF groups revealed an enrichment of terms related to T cell activation (Fig. 3E). KEGG enrichment analysis indicated that T cells were downregulated in pathways of atherosclerosis, dilated cardiomyopathy, and hypertrophic cardiomyopathy (Fig. 3F). To determine whether the T cells were modified by WRMs, we estimated WRM expression in the T cell subtypes. The differential expression of WRMs among T cell subtypes was as anticipated (Fig. 3G). The WRM scores of $CD8^+$ Temra and $CD8^+$ Tem were significantly higher in the NHF samples than in the HF samples (Fig. 3H). WRM also participated in the T cell differentiation trajectory (Fig. S2C). Thus, our findings demonstrated that cardiomyocytes interacted with $CD8^+$ Tem cells via the MIF signaling pathway and WRMs are closely associated with cardiac T cell dysregulation.

Macro-LYVE1 and Macro-MYL2 as CRMs are identified

Cardiac macrophages contribute to cardiac repair and remodeling post-injury [27, 47]. In this study, we extracted myeloid cells, employed scRNA-seq data for probing gene expression profiles of macrophages, and defined their heterogeneity in HF. The myeloid cells were divided into six distinct clusters: DC, Macro-IL1B, Macro-LYVE1, Macro-MYL2, Macro-SPP1, Mono-CD14, and Mono-CD16 (Fig. 4A). The Macro-LYVE1 and Macro-MYL2 populations were present in a higher percentage in the NHF samples than in the HF samples, suggesting that the two subtypes were predominantly present in the heart during the steady state (Fig. 4B). The heatmap demonstrated genes with high expression in each macrophage subtype (Fig. 4C). We observed that Macro-LYVE1 and Macro-MYL2 were characterized by the expression of lymphatic vessel endothelial hyaluronan receptor-1 (*LYVE1*), folate receptor 2 (*FOLR2*), mannose receptor C-type 1 (*MRC1*), C-C motif ligand 2 (*CCL2*), and coagulation factor XIIIA (*F13A1*, Fig. 4C), which resembled the signatures of cardiac tissue-resident macrophages [27, 48]. These results identified two CRM populations: Macro-LYVE1 and Macro-MYL2. Interestingly, Macro-MYL2 subtype exhibited elevated expression of cardiomyocyte structural genes, including *MYL2*, *TNNI3*, *TNNC1*, *TCAP*, and *TNNT2* (Fig. S3A), which were considered to constitute molecular diagnostic markers for hypertrophic cardiomyopathy [49]. Hence, we focused on Macro-MYL2 cells to investigate the effects of CRMs on HF.

Macro-MYL2 differs from Macro-LYVE1 in function enrichment and differentiation trajectory

To determine the activating transcription factors (TFs) and functional enrichment of these myeloid cell subtypes, we performed SCENIC analysis and GSVA enrichment analysis. Among the myeloid cell subtypes, Macro-LYVE1 and Macro-MYL2 exhibited comparable transcriptional pattern activation, with T cell acute lymphocytic leukemia 2 (*TAL2*) and nuclear factor I B (*NFIB*) being specially activated in both subtypes (Fig. S3B). Macro-MYL2 cells were significantly enriched with myogenesis and suppressed in a set of immune response-associated pathways such as IL6/JKT/STAT3 signaling, IL2/JKT/STAT5 signaling, inflammatory response, and interferon gamma/alpha response, as demonstrated in Fig. 4D. Macro-LYVE1 cells were activated in the processes of protein secretion, bile acid metabolism, and coagulation. Macro-IL1B cells evidently exhibited characteristics of inflammatory response and apoptosis, including the presence of TNFA signaling

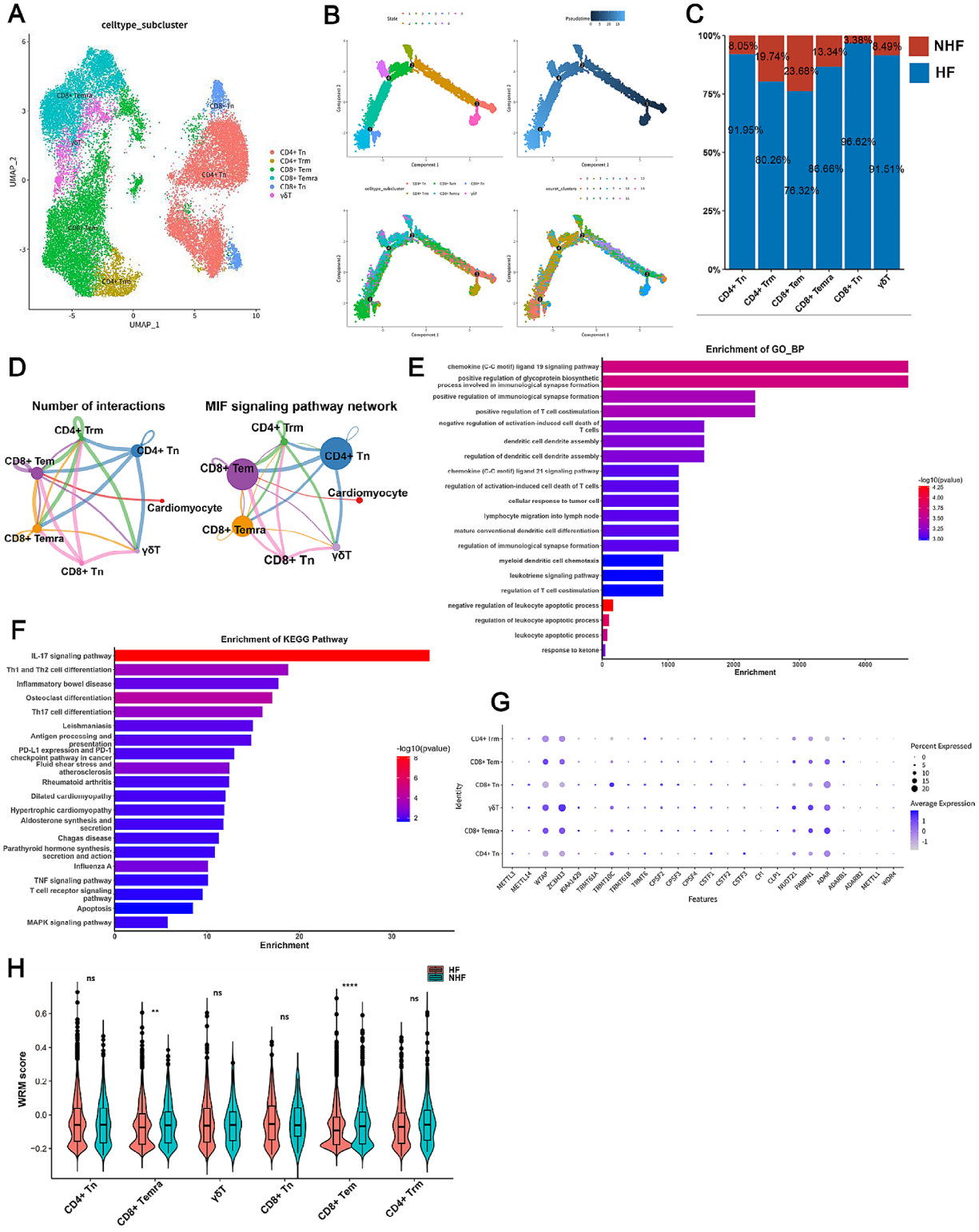

Fig. 3 WRMs are associated with T cells in heart. (**A**) T cell subtype annotation by using the UMAP plot. (**B**) The Monocle prediction of the T cell subtype developmental trajectory. (**C**) Bar plot for T cell subtypes revealed that the percentage of T cell subtypes in the HF samples was higher than in the NHF samples. (**D**) Cell-cell communication among T cell subtypes. (**E**) GO term analysis revealed the functional enrichment of upregulated DEGs in T cells between the HF and NHF groups. (**F**) KEGG analysis revealed the functional enrichment of downregulated DEGs in T cells between the HF and NHF groups. (**G**) Expression of WRMs in the individual T cell subtypes. (**H**) WRM score expressing profile in individual T cell subtypes in HF and NHF samples. ns = not significant, $*p < 0.05$, $**p < 0.01$, and $***p < 0.001$

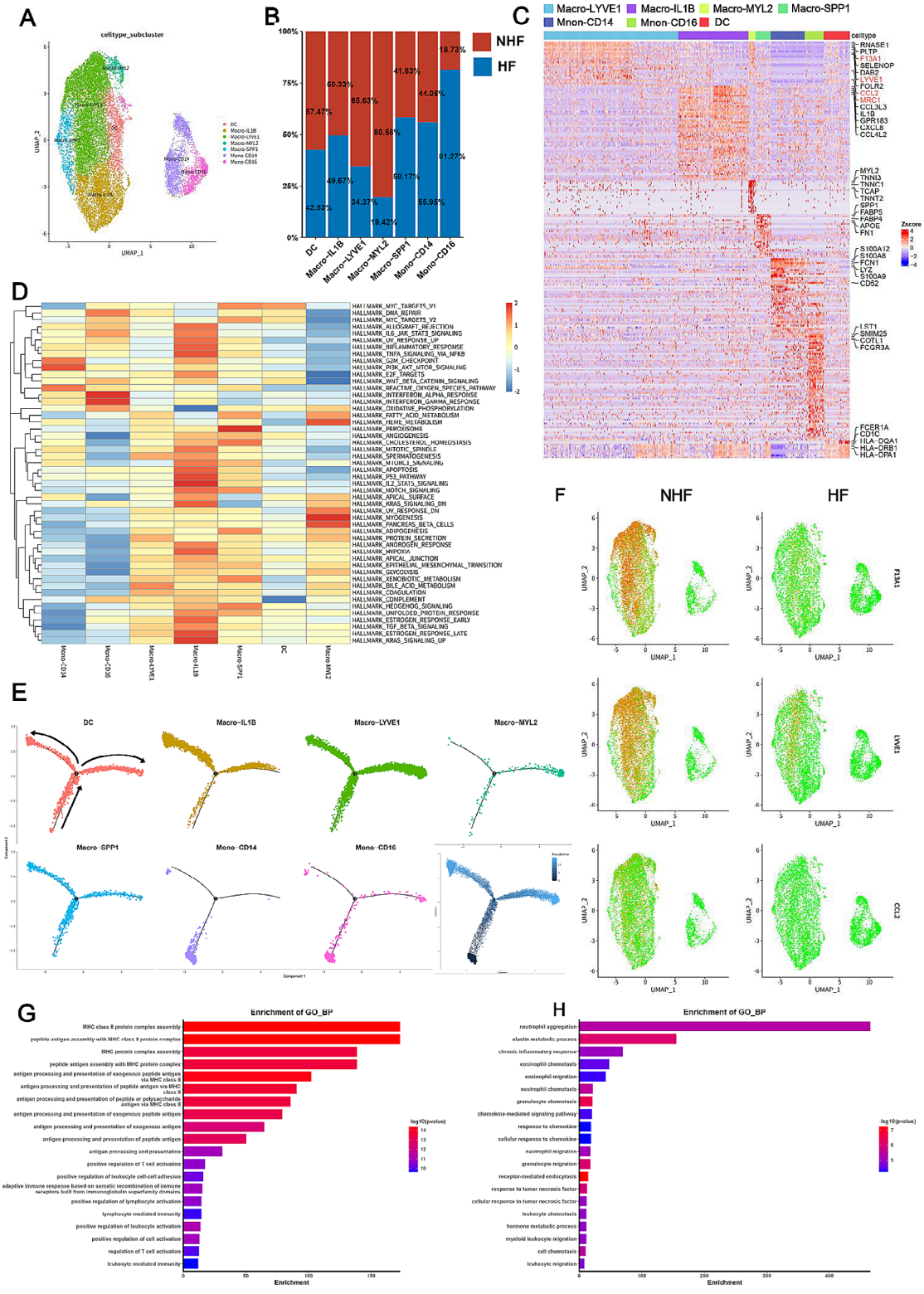

Fig. 4 Heterogeneous myeloid cell subtypes in HF. (**A**) Myeloid cell annotation by using the UMAP plot. (**B**) Bar plot showed the relative proportion of each myeloid cell subtype in HF and NHF samples. (**C**) Heatmap showing marker genes with exemplar genes and subtype annotations labeled in myeloid cell subtypes. (**D**) GSVA analysis of HALLMARK pathways of individual myeloid cell subtypes. (**E**) Trajectory analysis revealed myeloid cell subtypes with distinct differentiation patterns. (**F**) Expression of signature genes of CRMs between the HF group and NHF group. (**G** and **H**) GO functional enrichment analysis for DEGs between the HF and NHF groups demonstrated upregulated DEG-related terms (**G**) and downregulated DEG-related terms (**H**), respectively

via NFκB, interferon alpha/gamma response, IL6/JKT/STAT3 signaling, as well as apoptosis and the p53 pathway (Fig. 4D). The Macro-SPP1 cells exhibited an activation in lipid metabolism, which included fatty acid metabolism, cholesterol homeostasis, and adipogenesis (Fig. 4D). Monocytes from peripheral blood can differentiate into DCs and macrophages [50]. During pseudotime analysis, the undifferentiated monocytes, Mono-CD14 and Mono-CD16 cells, were located at the onset of the pseudotime trajectory. The mature populations of DC, Macro-IL1B, and Macro-SPP1 appeared at the early stage of myeloid cell development (Fig. 4E). Macro-LYVE1 and Macro-MYL2 cells were classified as resident macrophages; however, their differentiation trajectories were distinct. Macro-LYVE1 differentiated along the trajectory, while Macro-MYL2 primarily appeared as mature macrophages at the terminal of the pseudotime trajectory (Fig. 4E). DEG analysis was performed to examine the differential factors and pathways in macrophage subtypes between the HF and NHF groups (Fig. S3C). Interestingly, we noticed that the expression of several DEGs, including *F13A1*, *LYVE1*, and *CCL2*, was downregulated in the HF group (Fig. S3C), and downregulation of *F13A1*, *LYVE1*, and *CCL2* occurred mainly in the Macro-MYL2 and Macro-LYVE1 subtypes (Fig. 4F). The F13A1 and LYVE1 generated by CRMs are associated with cardiovascular protection and cardiac lymphatics, respectively [48, 51]. Additionally, the CCL2 produced by CRMs triggers the recruitment of inflammatory monocytes, thereby amplifying vascular inflammation [52]. The downregulation of *F13A1*, *LYVE1*, and *CCL2* in the Macro-MYL2 and Macro-LYVE1 cells may impact macrophage-based regulation of cardiovascular and cardiac lymphatic remodeling in HF. Upon comparison with the NHF group, enrichment analysis demonstrated that the upregulated DEGs in the HF group were primarily involved in antigen processing and presentation via MHC class II and T cell activation (Fig. 4G). Conversely, the chemokine- and neutrophil-associated pathways were enriched in the downregulated DEGs (Fig. 4H). Thus, our results illustrated the heterogeneity of myeloid cell subtypes and revealed that Macro-MYL2 cells were specifically activated during myogenesis and were distinct from the differentiation trajectory of Macro-LYVE1 cells.

TRMT10C participates in Macro-MYL2 subtype differentiation

To determine if any strong associations existed between WRMs and myeloid cells in the HF development, we assessed WRM expression in the different subtypes. Figure 5A illustrates the distinct expression of WRM in myeloid cell subtypes. In addition, the WRM scores in the Mono-CD14, Mono-CD16, Macro-LYVE1, and Macro-IL1B subtypes were significantly higher in the NHF group than in the HF group (Fig. S3D). The WRM gene expression was subsequently plotted to track variations across different myeloid cell states, which demonstrated the participation of WRM in the myeloid cell differentiation process (Fig. 5B). *TRMT10C* was responsible for the m1A modification of mitochondrial tRNA and mRNA [53]. The trajectory of Macro-MYL2 differentiation was characterized by a gradual increase in *TRMT10C* expression (Fig. 5B). We also discovered elevated *TRMT10C* expression in the NHF group compared to the HF group (Fig. S3E), consistent with the alterations in Macro-MYL2 abundance (Fig. 4B). Subsequently, *Trmt10c* was overexpressed in cardiac macrophages of mice (Fig. 5C and D), which resulted in a significant elevation of the $MYL2^+$ macrophage population (Fig. 5E). These results demonstrated *TRMT10C* involvement in Macro-MYL2 differentiation.

Identification of immune microenvironment in HF based on the bulk RNA-seq data

To further investigate the regulatory roles of WRM in the immune microenvironment in HF, we employed the bulk RNA-seq data from the GSE141910 dataset, which included 200 HF samples and 166 NHF samples [43]. DEG analysis was initially performed between the HF and NHF samples, and a total of 901 DEGs were detected, including 624 upregulated DEGs and 277 downregulated DEGs (Fig. S4A). The GO enrichment analysis revealed that the upregulated genes were actively involved in immune and fibrotic responses, including immune response-activating cells, T cell differentiation, regulation of T cell activation, mononuclear cell differentiation, and lymphocyte differentiation, as well as collagen fibril organization and extracellular matrix organization (Fig. 6A). Moreover, the DEGs involved in macrophage regulation and acute response were downregulated in HF. This included DEGs engaged in the positive regulation of macrophage-derived foam cell differentiation, macrophage activation, acute-phase response, and acute inflammatory response (Fig. 6B). We also evaluated the infiltrating level of immune cells (Fig. S4B). The infiltrating levels of several subtypes, including $CD4^+$ Tn, $CD8^+$ Temra, $CD8^+$ Tem, and DC, were significantly higher in HF samples than in NHF samples (Fig. 6C). Conversely, the levels of $CD4^+$ Trm, Macro-CD14, Macro-IL1B, and Macro-MYL2 cells were significantly higher in NHF samples than in HF samples. We also found that changes in abundance of $CD4^+$ Tn, $CD8^+$ Temra, $CD8^+$ Tem, and Macro-MYL2 cells were consistent with the scRNA-seq data results (Figs. 3C, 4B, and 6C). Upon cell-chat analysis, we observed that these immune cell subtypes exhibited a close interaction with each other, with DC and Macro-MYL2 being the most negatively correlated

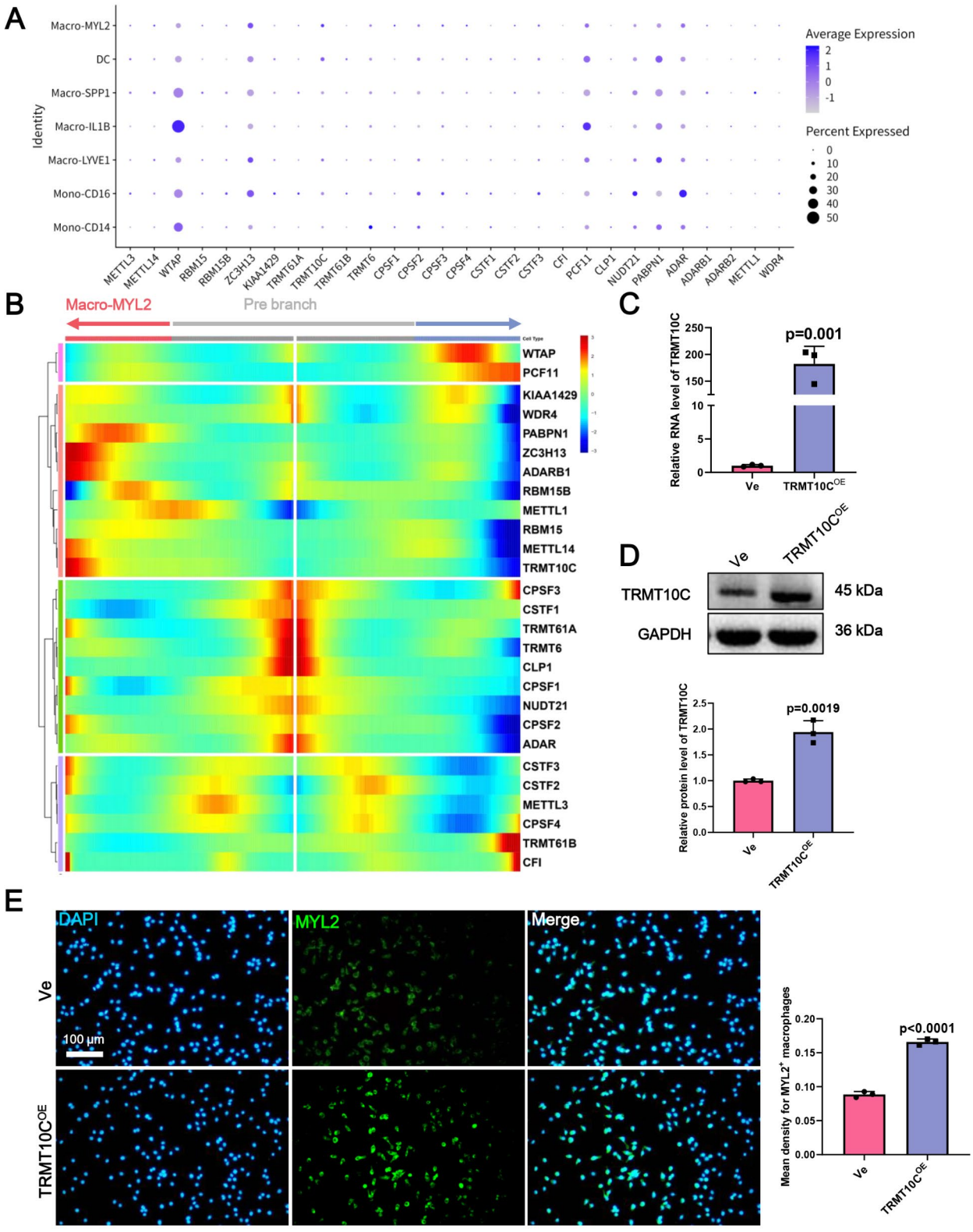

Fig. 5 WRMs contribute to macrophage differentiation. (**A**) Bubble plot illustrating the expression profile of WRM in each macrophage subtype. (**B**) Heatmap of WRM expression profile along the pseudotime of branch 1 during the macrophage differentiation. (**C**) qRT-PCR identified *Trmt10c* expression in cardiac macrophages of mice. (**D**) Western blot identified Trmt10c level in cardiac macrophages of mice. (**E**) Representative fluorescent images of MYL2 in cardiac macrophages of mice (×20). The Image Pro Plus software was used to measure the green fluorescence intensity, which represents the ratio of $MYL2^+$ macrophages. "Ve" represents the vector control with an empty plasmid, and "$TRMT10C^{OE}$" indicates the vector carrying overexpression of the *Trmt10c* gene

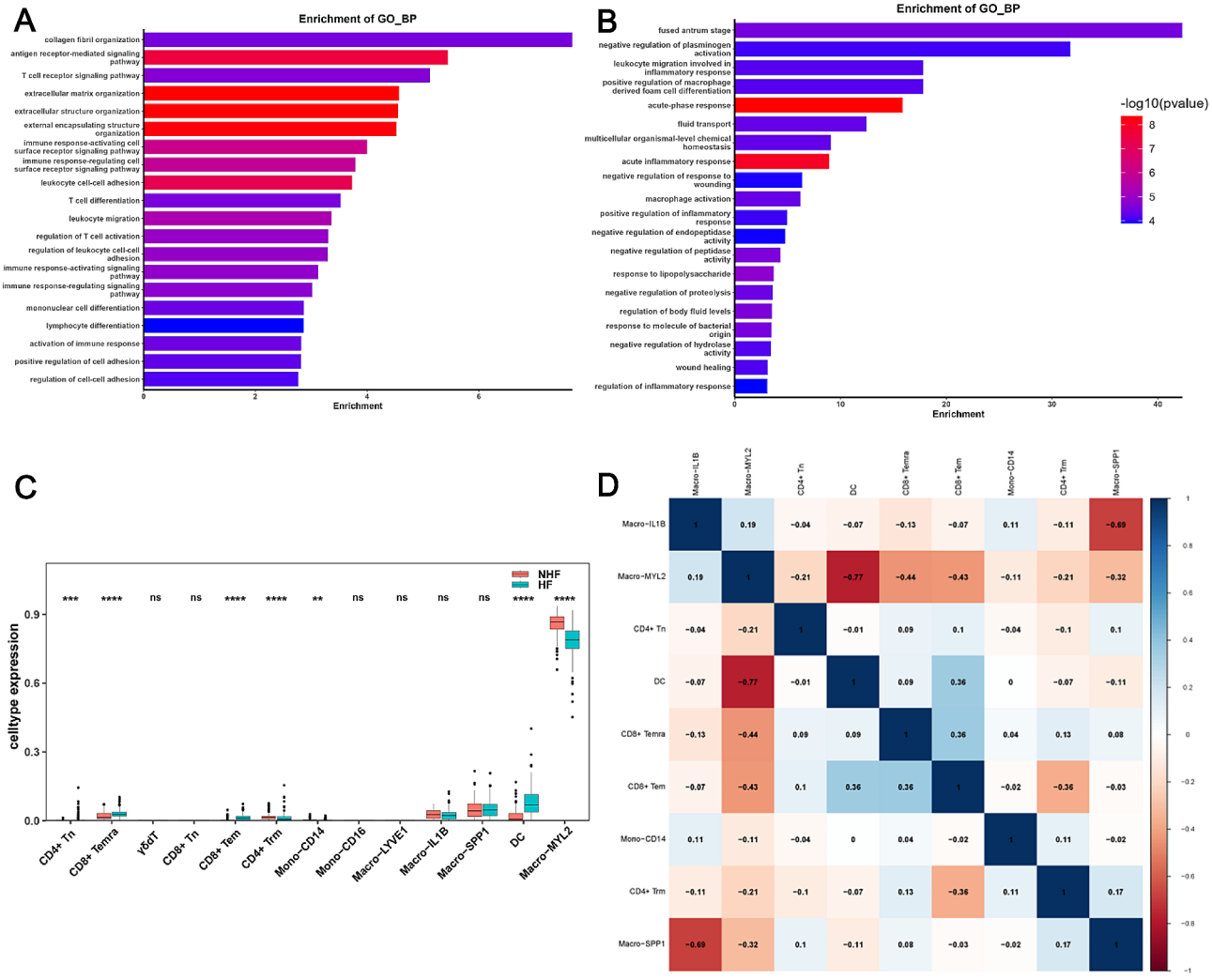

Fig. 6 Bulk RNA-seq data reveals an immune dysregulation in HF. (**A**) and (**B**) GO functional enrichment analysis was performed for DEGs between the HF and NHF groups based on bulk RNA-seq data that showed GO terms related to upregulated DEGs (**A**) and downregulated DEGs (**B**), respectively. (**C**) The infiltrating level of immune cells in samples from bulk RNA-seq data. ns = not significant, *$p < 0.05$, **$p < 0.01$, and ***$p < 0.001$. **D** Correlations between the immune cell subtypes in samples from bulk RNA-seq data were visualized by heatmap, and the most positive (blue) or negative correlation (red) between immune cell-immune cell pairs were marked with different colors

(Fig. 6D). Together, these findings further confirmed that the immune response was dysregulated in HF.

RNA modification writers not only interacted with immune cells, but also with each other

We compared the WRM alterations between normal and HF samples to determine whether HF influenced WRM expression. The findings revealed that the expression of most of the writers varied in HF (Fig. 7A–E). Specifically, compared to the NHF samples, the expression of most of the WRMs was significantly higher in the HF samples. This included cleavage and polyadenylation specificity factor (*CPSF2*), pre-mRNA cleavage complex 2 protein (*PCF11*), *TRMT10C*, Wilms' tumor 1-associated protein (*WTAP*), and WD repeat domain 4 (*WDR4*, Fig. 7A–E). To explore the relationship between writers and immune cells, we assessed their pairwise correlations. The results indicated that $CD8^+$ Tem, $CD8^+$ Temra, and $CD4^+$ Tn exhibited a more negative correlation with WRMs (Fig. 7F). Additionally, the 28 writers in the HF samples engaged in a unique crosstalk that resulted in a positive correlation between the WRM within the same category and a significant correlation between various types of WRM (Fig. 7G). Our results revealed that the WRMs interacted with immune cells and with one another.

Unsupervised cluster analysis for HF samples by WRM clustering

The crosstalk among the writers was important for generating different RNA modification patterns between individual HF samples. Thus, based on the WRM expression, we conducted unsupervised consensus clustering

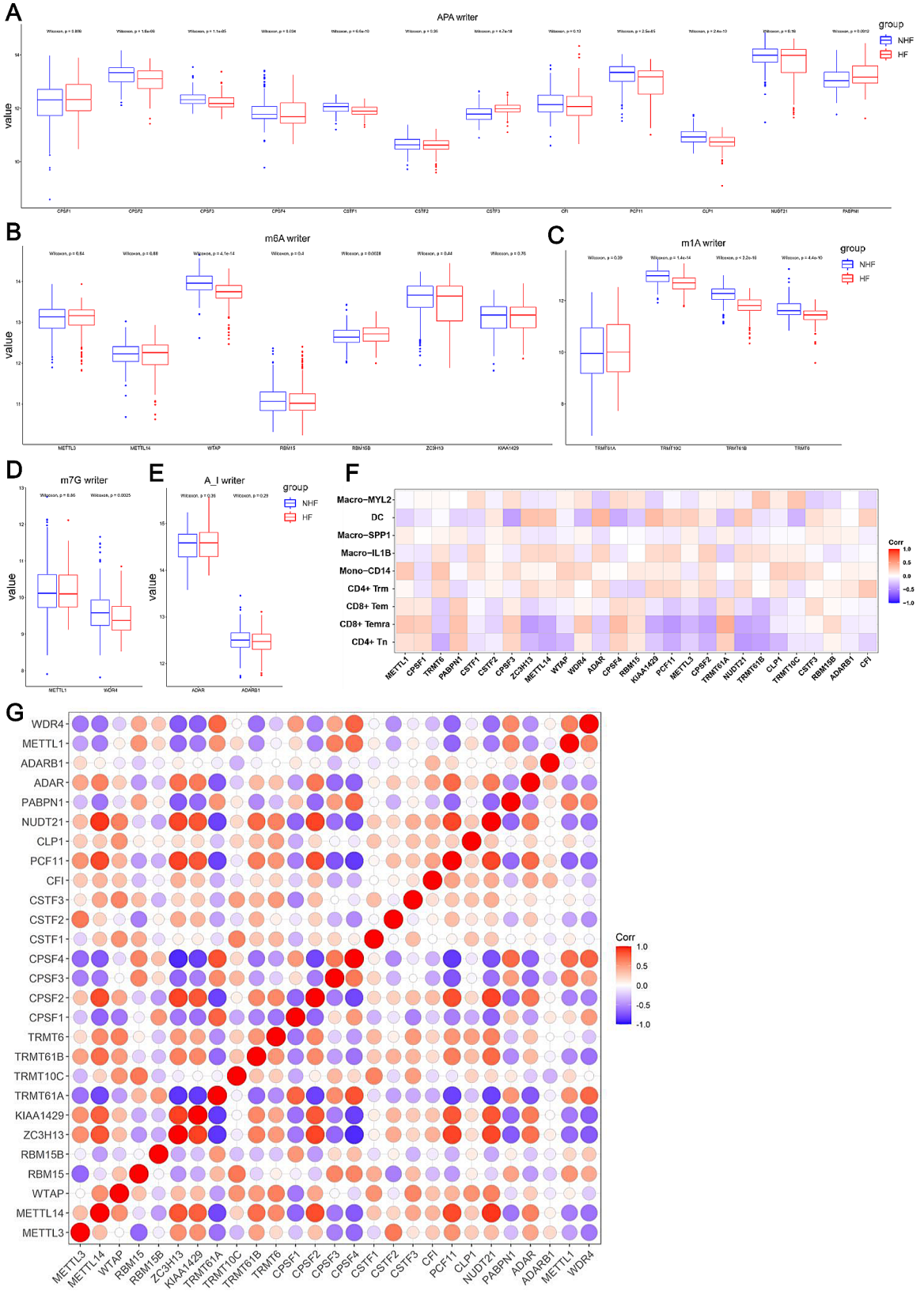

Fig. 7 Differential expression and relevant analysis of WRMs in HF samples. (**A–E**) Box plots showing the levels of the 28 writers between paired NHF (blue) and HF (red) samples in the bulk RNA-seq data, including writers of APA (**A**), m6A (**B**), m1A (**C**), m7G (**D**), and A-I (**E**). **F** Heatmap revealed a correlation between WRMs and immune cells in the bulk RNA-seq data. (**G**) Heatmap showed positive (red) and negative (blue) correlations among the 28 writers in HF samples from bulk RNA-seq data

analysis for HF samples to further investigate RNA modification patterns in HF (Fig. S5A–C). The clustering results demonstrated that k=2 was an appropriate selection, indicating that HF samples were accurately divided into two types: WRM type 1 and WRM type 2 (Fig. 8A). A GSVA enrichment analysis was conducted to further define the WRM type 1 and WRM type 2 phenotypes. As shown in Fig. 8B, WRM type 2 was significantly enriched in myogenesis, PI3K/AKT/MTOR signaling, the p53 pathway, glycolysis, reactive oxygen species, oxidative phosphorylation, DNA repair, and fatty acid metabolism. For WRM type 1, cell cycle-related pathways were activated, such as E2F targets, G2M checkpoints, and the mitotic spindle (Fig. 8B). Furthermore, DEG analysis results revealed alterations in 4,509 DEGs between WRM type 1 and WRM type 2, including 2,212 upregulated genes and 2,297 downregulated genes (Fig. S5D). The KEGG enrichment analysis revealed that, compared with type 2 WRMs, upregulated DEGs of type 1 WRMs were significantly enriched in arrhythmogenic right ventricular cardiomyopathy and actin cytoskeleton regulation (Fig. 8C). DEGs that are involved in oxidative phosphorylation, diabetic cardiomyopathy, cardiac muscle contraction, phagosomes, and endocytosis were downregulated, as illustrated in Fig. 8D.

To better understand immune-related characteristics in WRM type 1 and WRM type 2, we evaluated the immune cell infiltration within the two WRM types (Fig. S5E). We observed that the infiltration level of immune cell subtypes, including $CD4^+$ Tn, $CD8^+$ Temra, Macro-SPP1, and Macro-MYL2, was significantly higher in WRM type 2 than in WRM type 1. However, $CD4^+$ Trm, Mono-CD14, Macro-IL1B, and DC were significantly enriched in WRM type 1 (Fig. 8E). Furthermore, the expressions of RNA modification regulators demonstrated substantial differences in WRM type 1 and WRM type 2 (Fig. S5F). In general, these results indicated that two WRM-related regulatory patterns were present in HF samples, and the two types exhibited distinct immune-related characteristics.

Discussion

Inflammation dysregulation is a prevalent underlying contributor to the risk factors associated with HF, and the immune microenvironment is closely correlated with RNA modification regulators in the development of HF [38, 54]. Our results revealed immune response dysregulation and a global landscape of RNA modification writers in the HF immune microenvironment using scRNA-seq and bulk RNA-seq data. We identified a myogenesis-related CRM population, termed Macro-MYL2, which excessively expresses cardiomyocyte structural genes. Additionally, WRM TRMT10C plays an important role in Macro-MYL2 subtype differentiation. Our findings highlight the impact of WRMs on the immune microenvironment of HF and identify potential targets for improving diagnostic and therapeutic strategies for HF.

This study revealed noticeable differences in the immune environment between HF and normal patients, consistent with previous studies [55]. In the early stage of cardiac injury, reparative or anti-inflammatory responses are essential for minimizing myocardial damage, promoting healing, and preventing scar formation. Conversely, an enhanced or persistent pro-inflammatory response can delay the reparative macrophage-mediated repair response and exacerbate adverse ventricular remodeling [56], suggesting the dual role of the immune response in the heart. Similarly, atherosclerosis is an immune-mediated inflammatory condition. Both immune cells and their secreted cytokines have a protective and pro-atherogenic effect on atherosclerotic plaques [57]. The polarization of the pro-inflammatory and anti-inflammatory macrophage phenotypes plays a pivotal role in HF development. For example, YAP/TAZ promotes the pro-inflammatory response by increasing IL6 expression in macrophages. Conversely, YAP/TAZ deletion results in impaired pro-inflammatory and enhanced reparative responses, leading to improved cardiac function [56]. Blocking TRPA1 also decreases the proportion of M2 macrophages and reduces profibrotic cytokine levels, thereby improving cardiac fibrosis [58]. Additionally, IL-34 can sustain NF-κB pathway activation to elicit elevated CCL2 expression, which contributes to $CCR2^+$ macrophage recruitment and polarization and subsequently exacerbates cardiac remodeling and HF post-ischemia/reperfusion [59]. These results underscore the critical function of macrophages in HF. In this study, the distribution and pseudotime trajectory of different subclusters within the same cell type exhibited differences between the HF and NHF samples. For instance, a higher proportion of Macro-LYVE1 and Macro-MYL2 subtypes were observed in the NHF samples than in the HF samples, in contrast with other macrophage subtypes. In addition, Mono-CD14 and Mono-CD16 cells were located at the beginning of the pseudotime trajectory, and the Macro-IL1B and Macro-SPP1 subtypes appeared at the early stage of myeloid cell development. Thus, the immune system strictly regulates the differentiation of cardiac macrophages in response to HF development.

Our results revealed that RNA modification writers were closely associated with immune dysregulation in HF. Abnormal RNA modification in immune cells have been identified in cardiovascular disease [60]. For example, the group with a higher insulin-like growth factor-binding protein 3 (IGFBP3) level exhibits more enriched immune-related pathways and highly infiltrated immune cells in comparison to the low IGFBP3 group [54]. In

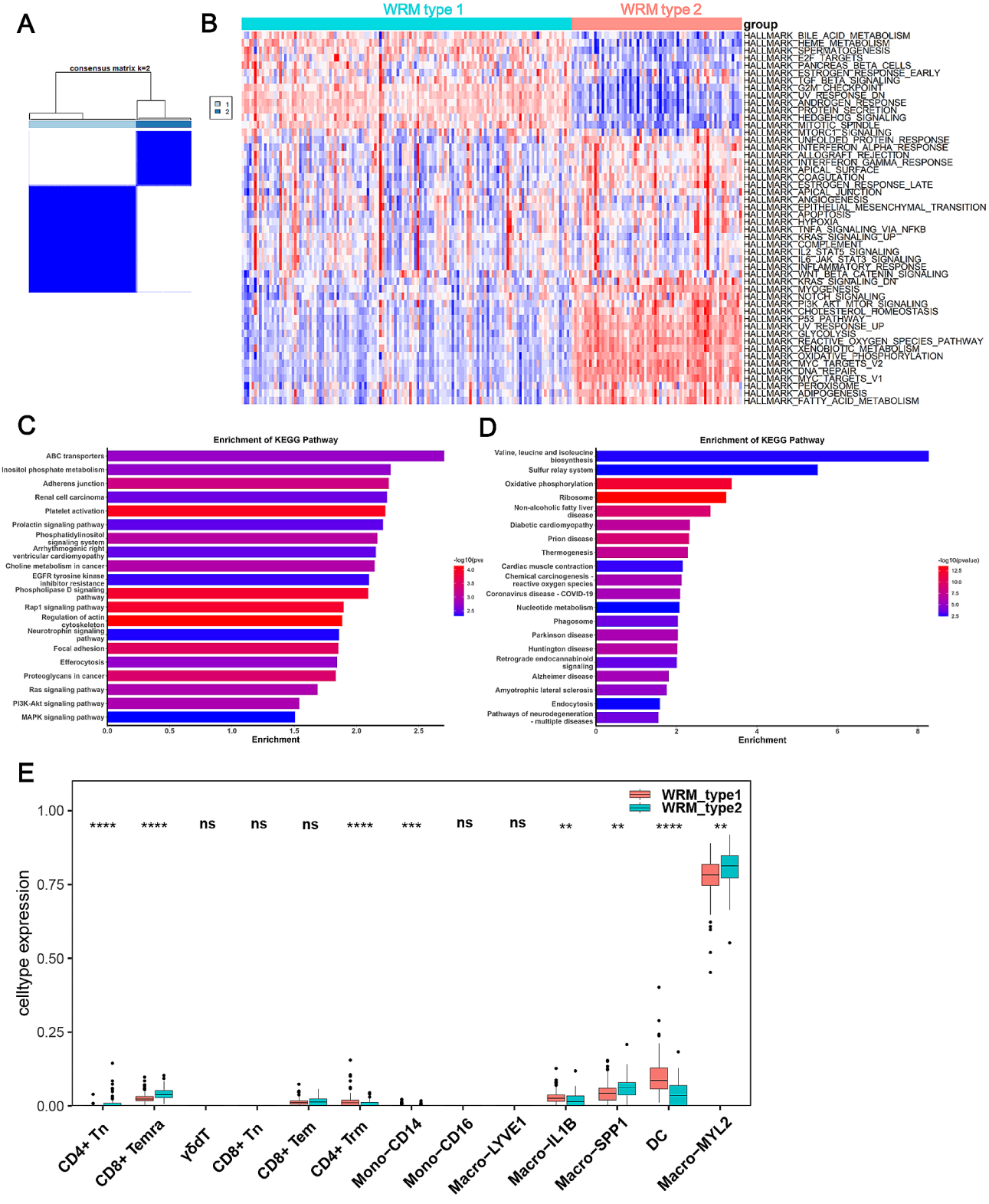

Fig. 8 Identification of two distinct WRM modification types across HF samples. (**A**) Consensus matrix heatmap defining two WRM types (k = 2) and their correlation area. (**B**) Heatmap revealed significant pathways of two distinct WRM types. (**C** and **D**) Enrichment of KEGG pathway showed significant pathways of upregulated DEGs (**C**) or downregulated DEGs (**D**) between WRM type 1 and WRM type 2. (**E**) Differential expression of immune cells in two distinct WRM types

addition, the differentially expressed m7G regulators are closely associated with a diverse array of immune cell infiltrations and expression alterations of immune-related functions in HF. Multiple m7G regulators have been identified as diagnostic signatures for HF [38]. In our study, WRM was differentially expressed in cardiac immune cells. The WRM score of certain immune cells exhibited significant differences between the HF and NHF samples, with the NHF samples exhibiting higher WRM scores. This indicates that RNA modification level is a critical factor in immune cell infiltration. RNA modification regulators can regulate immune responses via multiple signaling pathways. One study reports that m6A regulator expression affects vascular cell adhesion molecule 1 expression and subsequently influences immune cell infiltration via the Wnt signaling pathway in HF [61]. FTO knockdown in rat cardiomyocytes upregulates the expression of pro-inflammatory cytokines, resulting in hypermethylation of IL-6 and TNF-α mRNA transcripts [62]. Our study revealed that WRM-related immune cells were activated in pathways related to interferon gamma/alpha, IL6/JAK/STAT3 signaling, and IL2/JAK/STAT5 signaling. Thus, future research can further explore the role of WRM in the signaling pathway of immune cells.

In this study, we identified two major resident macrophage populations in the heart, namely the Macro-LYVE1 and Macro-MYL2 subtypes. CRMs can be divided into $CCR2^{-}$ and $CCR2^{+}$ subtypes, which are derived from embryonic and adult hematopoietic lineages, respectively. $CCR2^{+}$ resident macrophages can be derived from blood $CCR2^{+}$ monocytes [63, 64]. Local proliferation of $CCR2^{-}$ macrophages and recruitment of blood monocytes both contribute to cardiac macrophage expansion [64]. Recent studies reveal a significant reduction in certain resident macrophage populations in heart tissue during the early stages of cardiovascular disease. However, they are subsequently restored to facilitate repair after myocardial injury [65, 66]. This study revealed that Macro-LYVE1 and Macro-MYL2 abundance was reduced in HF samples, and resident macrophage signatures such as *LYVE1*, *CCL2*, and *F13A1* in both subtypes were significantly downregulated compared with the NHF samples. We hypothesize that the Macro-LYVE1 and Macro-MYL2 subtypes are beneficial for the heart and that the local proliferation of macrophages and the recruitment of blood monocytes are limited in HF patients who experienced cardiac dysfunction for a prolonged period, thereby promoting adverse cardiac remodeling. Interestingly, the Macro-LYVE1 and Macro-MYL2 cells exhibited significant differences in pathway enrichment, suggesting that these two CRM subtypes perform different functions in the heart. Furthermore, pseudotime analysis demonstrated that Macro-LYVE1 cells developed along the trajectory, and Macro-MYL2 cells primarily appeared at the terminal phase of the pseudotime trajectory. This indicates that Macro-LYVE1 and Macro-MYL2 cells may originate from different cell lineages.

CRMs can stimulate angiogenesis and inhibit fibrosis in response to cardiac pressure overload [27]. They are responsible for the efficient clearance of dysfunctional mitochondria and the degradation of apoptotic cardiomyocytes for tissue repair [65, 67]. Macro-MYL2 cells constitute a unique CRM population characterized by the expression of cardiomyocyte structural genes. These genes play essential roles in cardiac contractile function [49, 68]. Macro-MYL2 cells also actively involved in the myogenesis pathway and were known to downregulate immune response-related genes. This suggests that Macro-MYL2 may respond to HF by engaging in cardiac remodeling rather than immunity. Tracking gene expression changes of WRM across myeloid cell states revealed a close relationship between RNA modification and Macro-MYL2 differentiation. Previous studies have demonstrated the regulatory roles of RNA modification regulators in macrophage polarization. For instance, the polarization of macrophages is linked to YTHDF3, and the polarization of macrophage M1 induced by lipopolysaccharide/IFN-γ can be impaired by YTHDF3 suppression [69]. In macrophages, METTL3 upregulation also drives M1 macrophage polarization, and deficient METTL3 inhibits macrophage activation [70, 71]. METTL14 expression is increased in coronary heart disease, but METTL14 knockout significantly reduces macrophage-based inflammatory responses and atherosclerotic plaque development [72]. The above studies highlight the importance of WRMs in macrophage polarization. Interestingly, the process of Macro-MYL2 subtype differentiation was accompanied by enhanced expression of *TRMT10C*, and the proportion of $MYL2^{+}$ macrophages was increased by *Trmt10c* overexpression in cardiac macrophages. *TRMT10C* is responsible for m1A modification of mitochondrial mRNA and tRNA [73, 74], suggesting that TRMT10C may regulate Macro-MYL2 subtype differentiation in the heart via m1A modification of mitochondrial mRNA or tRNA. Further investigation is required to elucidate the mechanism by which TRMT10C modulates the Macro-MYL2 subtype through m1A modification of RNA.

Conclusion

In this study, we comprehensively demonstrated the impact of WRMs on the immune microenvironment in HF by using scRNA-seq and bulk RNA-seq data. We also identified a myogenesis-related population of CRMs, termed Macro-MYL2, characterized by increased expression of cardiomyocyte structural genes and regulated

by *TRMT10C*. Our results provide a novel approach for identifying biomarkers for HF treatment and diagnosis.

Abbreviations

HF	Heart Failure
WRM	Writers of RNA Modification
NHF	Non-Heart Failure
SGLT2	Sodium/Glucose Cotransporter 2
NK	Natural Killer
scRNA-seq	Single-Cell RNA Sequencing
m6A	N6-methyladenosine
m1A	N1-methyladenosine
m7G	N7-methylguanosine
APA	Alternative Polyadenylation
A-I	Adenosine-to-Inosine
GEO	Gene Expression Omnibus
NHF	Non-HF
UMIs	Unique Molecular Identifiers
UMAP	Uniform Manifold Approximation and Projection
SCENIC	Single-Cell Regulatory Network Inference and Clustering
GSVA	Gene-Set Variation Analysis
GO	Gene Ontology
KEGG	Kyoto Encyclopedia of Genes and Genomes
ssGSEA	single-sample Gene-Set Enrichment Analysis
SMC	Smooth Muscle Cell
Tn cells	naïve T cells
Trm cells	Tissue resident memory cells
Tem cells	Effector Memory T cells
Temra	Effector memory cells re-expressing CD45RA
MIF	Migration Inhibitory Factor
DC	Dendritic Cell
TFs	Transcription Factors
METTL3	Methyltransferase-Like 3
MYL2	Myosin Light Chain 2
TNNI3	Troponin I3
TNNC1	Troponin C type 1
TCAP	Teneurin C-Terminal Associated Peptides
TNNT2	Troponin T2
LYVE1	Lymphatic Vessel Endothelial Hyaluronan Receptor-1
FOLR2	Folate Receptor 2
MRC1	Mannose Receptor C-type 1
CCL2	C-C Motif Ligand 2
F13A1	Coagulation Factor XIIIA
TAL2	T-cell Acute Lymphocytic Leukemia 2
NFIB	Nuclear Factor I B
METTL14	Methyltransferase-like 14
TRMT10C	TRNA Methyltransferase 10 C
CPSF2	Cleavage and Polyadenylation Specificity Factor
PCF11	Pre-mRNA Cleavage Complex 2 Protein\
WTAP	Wilms'Tumor 1-Associated Protein
WDR4	WD Repeat Domain 4

Supplementary Information

The online version contains supplementary material available at https://doi.org/10.1186/s12872-024-04080-x.

Supplementary Material 1

Supplementary Material 2

Supplementary Material 3

Supplementary Material 4

Supplementary Material 5

Supplementary Material 6

Acknowledgements
Not applicable.

Author contributions
YLY and XWL contributed equally to this study. YLY and XWL were responsible for overall data analysis and wrote the manuscript. HBC, QDT, and YHL were responsible for the statistical analysis and correction of each data. JYX and JJX were responsible for the study design, revised the manuscript and obtained funding support. YLY and XWL should be considered joint first authors. All the authors read and approved the final form of the manuscript.

Funding
This research was supported by the Science and Technology Projects in Guangzhou [2023A03J0252].

Data availability
The datasets used and analyzed during the current study are available from publicly available GEO database GSE145154 and GSE141910. The links are as follows: GSE145154: https://www.ncbi.nlm.nih.gov/geo/query/acc.cgi?acc=GSE145154. GSE141910: https://www.ncbi.nlm.nih.gov/geo/query/acc.cgi?acc=GSE141910.

Declarations

Ethics approval and consent to participate
Our analysis is based on prior research and does not require ethical approval from ethical review board or informed consent from patients.

Consent for publication
Not applicable.

Competing interests
The authors declare that they have no competing interests.

Author details
[1]First Department of Cardiology, the affiliated Guangdong Second Provincial General Hospital, NO. 466, Xingang Middle Road, Haizhu District, Guangzhou City, China

Received: 9 January 2024 / Accepted: 29 July 2024
Published online: 16 August 2024

References

1. McMurray JJ, Pfeffer MA. Heart failure. Lancet. 2005;365(9474):1877–89.
2. Qian K, Tang J, Ling YJ, Zhou M, Yan XX, Xie Y, Zhu LJ, Nirmala K, Sun KY, Qin ZH, et al. Exogenous NADPH exerts a positive inotropic effect and enhances energy metabolism via SIRT3 in pathological cardiac hypertrophy and heart failure. EBioMedicine. 2023;98:104863.
3. Baman JR, Ahmad FS. Heart failure. JAMA. 2020;324(10):1015.
4. Tanai E, Frantz S. Pathophysiology of heart failure. Compr Physiol. 2015;6(1):187–214.
5. Lidgard B, Bansal N, Zelnick LR, Hoofnagle AN, Fretts AM, Longstreth WT Jr., Shlipak MG, Siscovick DS, Umans JG, Lemaitre RN. Evaluation of plasma sphingolipids as mediators of the relationship between kidney disease and cardiovascular events. EBioMedicine. 2023;95:104765.
6. Yu Y, Liu J, Zhang L, Ji R, Su X, Gao Z, Xia S, Li J, Li L. Perceived Economic Burden, Mortality, and Health Status in patients with heart failure. JAMA Netw Open. 2024;7(3):e241420.
7. Vaduganathan M, Claggett BL, Jhund PS, Cunningham JW, Pedro Ferreira J, Zannad F, Packer M, Fonarow GC, McMurray JJV, Solomon SD. Estimating lifetime benefits of comprehensive disease-modifying pharmacological therapies in patients with heart failure with reduced ejection fraction: a comparative analysis of three randomised controlled trials. Lancet. 2020;396(10244):121–8.
8. McMurray JJ, Packer M, Solomon SD. Neprilysin inhibition for heart failure. N Engl J Med. 2014;371(24):2336–7.
9. Khan MN, Soomro NA, Naseeb K, Bhatti UH, Rauf R, Balouch IJ, Moazzam A, Bashir S, Ashraf T, Karim M. Safety and tolerability of Sacubitril/Valsartan in heart failure patient with reduced ejection fraction. BMC Cardiovasc Disord. 2023;23(1):133.

10. Chen HB, Yang YL, Meng RS, Liu XW. Indirect comparison of SGLT2 inhibitors in patients with established heart failure: evidence based on bayesian methods. ESC Heart Fail. 2023;10(2):1231–41.
11. Li J, Zhu C, Liang J, Hu J, Liu H, Wang Z, Guan R, Chow J, Yan S, Li L, et al. Cardiovascular benefits and safety of sotagliflozin in type 2 diabetes mellitus patients with heart failure or cardiovascular risk factors: a bayesian network meta-analysis. Front Pharmacol. 2023;14:1303694.
12. Kresoja KP, Unterhuber M, Wachter R, Rommel KP, Besler C, Shah S, Thiele H, Edelmann F, Lurz P. Treatment response to spironolactone in patients with heart failure with preserved ejection fraction: a machine learning-based analysis of two randomized controlled trials. EBioMedicine. 2023;96:104795.
13. Peng L, Song Z, Zhao C, Abuduwufuer K, Wang Y, Wen Z, Ni L, Li C, Yu Y, Zhu Y, et al. Increased Soluble Epoxide Hydrolase Activity positively correlates with mortality in heart failure patients with preserved ejection fraction: evidence from Metabolomics. Phenomics. 2023;3(1):34–49.
14. Rurik JG, Tombacz I, Yadegari A, Mendez Fernandez PO, Shewale SV, Li L, Kimura T, Soliman OY, Papp TE, Tam YK, et al. CAR T cells produced in vivo to treat cardiac injury. Science. 2022;375(6576):91–6.
15. Wang J, Zhu X, Wang S, Zhang Y, Hua W, Liu Z, Zheng Y, Lu X. Phosphoproteomic and proteomic profiling in post-infarction chronic heart failure. Front Pharmacol. 2023;14:1181622.
16. Petersen TB, de Bakker M, Asselbergs FW, Harakalova M, Akkerhuis KM, Brugts JJ, van Ramshorst J, Lumbers RT, Ostroff RM, Katsikis PD, et al. HFrEF subphenotypes based on 4210 repeatedly measured circulating proteins are driven by different biological mechanisms. EBioMedicine. 2023;93:104655.
17. Crnko S, Printezi MI, Zwetsloot PM, Leiteris L, Lumley AI, Zhang L, Ernens I, Jansen TPJ, Homsma L, Feyen D, et al. The circadian clock remains intact, but with dampened hormonal output in heart failure. EBioMedicine. 2023;91:104556.
18. Adamo L, Rocha-Resende C, Prabhu SD, Mann DL. Reappraising the role of inflammation in heart failure. Nat Rev Cardiol. 2020;17(5):269–85.
19. Halade GV, Lee DH. Inflammation and resolution signaling in cardiac repair and heart failure. EBioMedicine. 2022;79:103992.
20. Moskalik A, Niderla-Bielinska J, Ratajska A. Multiple roles of cardiac macrophages in heart homeostasis and failure. Heart Fail Rev. 2022;27(4):1413–30.
21. Lu Y, Xia N, Cheng X. Regulatory T cells in Chronic Heart failure. Front Immunol. 2021;12:732794.
22. Zouggari Y, Ait-Oufella H, Bonnin P, Simon T, Sage AP, Guerin C, Vilar J, Caligiuri G, Tsiantoulas D, Laurans L, et al. B lymphocytes trigger monocyte mobilization and impair heart function after acute myocardial infarction. Nat Med. 2013;19(10):1273–80.
23. Kologrivova I, Shtatolkina M, Suslova T, Ryabov V. Cells of the Immune System in Cardiac Remodeling: main players in resolution of inflammation and repair after myocardial infarction. Front Immunol. 2021;12:664457.
24. Anzai A, Anzai T, Nagai S, Maekawa Y, Naito K, Kaneko H, Sugano Y, Takahashi T, Abe H, Mochizuki S, et al. Regulatory role of dendritic cells in postinfarction healing and left ventricular remodeling. Circulation. 2012;125(10):1234–45.
25. Palladini G, Tozzi R, Perlini S. Cardiac mast cells in the transition to heart failure: innocent bystanders or key actors? J Hypertens. 2003;21(10):1823–5.
26. Martini E, Kunderfranco P, Peano C, Carullo P, Cremonesi M, Schorn T, Carriero R, Termanini A, Colombo FS, Jachetti E, et al. Single-cell sequencing of Mouse Heart Immune infiltrate in pressure overload-driven heart failure reveals extent of Immune activation. Circulation. 2019;140(25):2089–107.
27. Revelo XS, Parthiban P, Chen C, Barrow F, Fredrickson G, Wang H, Yucel D, Herman A, van Berlo JH. Cardiac Resident macrophages prevent fibrosis and stimulate angiogenesis. Circ Res. 2021;129(12):1086–101.
28. Han D, Xu MM. RNA modification in the Immune System. Annu Rev Immunol. 2023;41:73–98.
29. Chen H, Yao J, Bao R, Dong Y, Zhang T, Du Y, Wang G, Ni D, Xun Z, Niu X, et al. Cross-talk of four types of RNA modification writers defines tumor microenvironment and pharmacogenomic landscape in colorectal cancer. Mol Cancer. 2021;20(1):29.
30. Zhu ZM, Huo FC, Pei DS. Function and evolution of RNA N6-methyladenosine modification. Int J Biol Sci. 2020;16(11):1929–40.
31. Li J, Zhang H, Wang H. N(1)-methyladenosine modification in cancer biology: current status and future perspectives. Comput Struct Biotechnol J. 2022;20:6578–85.
32. Zhang LS, Liu C, Ma H, Dai Q, Sun HL, Luo G, Zhang Z, Zhang L, Hu L, Dong X, et al. Transcriptome-wide mapping of Internal N(7)-Methylguanosine methylome in mammalian mRNA. Mol Cell. 2019;74(6):1304–e13161308.
33. Elkon R, Ugalde AP, Agami R. Alternative cleavage and polyadenylation: extent, regulation and function. Nat Rev Genet. 2013;14(7):496–506.
34. Li JB, Church GM. Deciphering the functions and regulation of brain-enriched A-to-I RNA editing. Nat Neurosci. 2013;16(11):1518–22.
35. Berulava T, Buchholz E, Elerdashvili V, Pena T, Islam MR, Lbik D, Mohamed BA, Renner A, von Lewinski D, Sacherer M, et al. Changes in m6A RNA methylation contribute to heart failure progression by modulating translation. Eur J Heart Fail. 2020;22(1):54–66.
36. Dorn LE, Lasman L, Chen J, Xu X, Hund TJ, Medvedovic M, Hanna JH, van Berlo JH, Accornero F. The N(6)-Methyladenosine mRNA methylase METTL3 controls Cardiac Homeostasis and Hypertrophy. Circulation. 2019;139(4):533–45.
37. Li T, Zhuang Y, Yang W, Xie Y, Shang W, Su S, Dong X, Wu J, Jiang W, Zhou Y, et al. Silencing of METTL3 attenuates cardiac fibrosis induced by myocardial infarction via inhibiting the activation of cardiac fibroblasts. FASEB J. 2021;35(2):e21162.
38. Ma C, Tu D, Xu Q, Wu Y, Song X, Guo Z, Zhao X. Identification of m(7)G regulator-mediated RNA methylation modification patterns and related immune microenvironment regulation characteristics in heart failure. Clin Epigenetics. 2023;15(1):22.
39. Zheng PF, Zhou SY, Zhong CQ, Zheng ZF, Liu ZY, Pan HW, Peng JQ. Identification of m6A regulator-mediated RNA methylation modification patterns and key immune-related genes involved in atrial fibrillation. Aging. 2023;15(5):1371–93.
40. Li Z, Song Y, Wang M, Shen R, Qin K, Zhang Y, Jiang T, Chi Y. m6A regulator-mediated RNA methylation modification patterns are involved in immune microenvironment regulation of coronary heart disease. Front Cardiovasc Med. 2022;9:905737.
41. Zheng PF, Hong XQ, Liu ZY, Zheng ZF, Liu P, Chen LZ. m6A regulator-mediated RNA methylation modification patterns are involved in the regulation of the immune microenvironment in ischaemic cardiomyopathy. Sci Rep. 2023;13(1):5904.
42. Du L, Sun X, Gong H, Wang T, Jiang L, Huang C, Xu X, Li Z, Xu H, Ma L, et al. Single cell and lineage tracing studies reveal the impact of CD34(+) cells on myocardial fibrosis during heart failure. Stem Cell Res Ther. 2023;14(1):33.
43. Flam E, Jang C, Murashige D, Yang Y, Morley MP, Jung S, Kantner DS, Pepper H, Bedi KC Jr., Brandimarto J, et al. Integrated landscape of cardiac metabolism in end-stage human nonischemic dilated cardiomyopathy. Nat Cardiovasc Res. 2022;1(9):817–29.
44. Blanton RM, Carrillo-Salinas FJ, Alcaide P. T-cell recruitment to the heart: friendly guests or unwelcome visitors? Am J Physiol Heart Circ Physiol. 2019;317(1):H124–40.
45. Qi D, Hu X, Wu X, Merk M, Leng L, Bucala R, Young LH. Cardiac macrophage migration inhibitory factor inhibits JNK pathway activation and injury during ischemia/reperfusion. J Clin Invest. 2009;119(12):3807–16.
46. Miller EJ, Li J, Leng L, McDonald C, Atsumi T, Bucala R, Young LH. Macrophage migration inhibitory factor stimulates AMP-activated protein kinase in the ischaemic heart. Nature. 2008;451(7178):578–82.
47. Xu Y, Jiang K, Su F, Deng R, Cheng Z, Wang D, Yu Y, Xiang Y. A transient wave of Bhlhe41(+) resident macrophages enables remodeling of the developing infarcted myocardium. Cell Rep. 2023;42(10):113174.
48. Beckers CML, Simpson KR, Griffin KJ, Brown JM, Cheah LT, Smith KA, Vacher J, Cordell PA, Kearney MT, Grant PJ, et al. Cre/lox studies identify Resident macrophages as the Major Source of Circulating Coagulation Factor XIII-A. Arterioscler Thromb Vasc Biol. 2017;37(8):1494–502.
49. Melas M, Beltsios ET, Adamou A, Koumarelas K, McBride KL. Molecular diagnosis of hypertrophic cardiomyopathy (HCM): in the heart of Cardiac Disease. J Clin Med 2022, 12(1).
50. Boyette LB, Macedo C, Hadi K, Elinoff BD, Walters JT, Ramaswami B, Chalasani G, Taboas JM, Lakkis FG, Metes DM. Phenotype, function, and differentiation potential of human monocyte subsets. PLoS ONE. 2017;12(4):e0176460.
51. Bizou M, Itier R, Majdoubi M, Abbadi D, Pichery E, Dutaur M, Marsal D, Calise D, Garmy-Susini B, Douin-Echinard V, et al. Cardiac macrophage subsets differentially regulate lymphatic network remodeling during pressure overload. Sci Rep. 2021;11(1):16801.
52. Miyabe C, Miyabe Y, Bricio-Moreno L, Lian J, Rahimi RA, Miura NN, Ohno N, Iwakura Y, Kawakami T, Luster AD. Dectin-2-induced CCL2 production in tissue-resident macrophages ignites cardiac arteritis. J Clin Invest. 2019;129(9):3610–24.
53. Safra M, Sas-Chen A, Nir R, Winkler R, Nachshon A, Bar-Yaacov D, Erlacher M, Rossmanith W, Stern-Ginossar N, Schwartz S. The m1A landscape on cytosolic and mitochondrial mRNA at single-base resolution. Nature. 2017;551(7679):251–5.

54. Li Y, Zhang W, Dai Y, Chen K. Identification and verification of IGFBP3 and YTHDC1 as biomarkers associated with immune infiltration and mitophagy in hypertrophic cardiomyopathy. Front Genet. 2022;13:986995.
55. Li S, Ge T, Xu X, Xie L, Song S, Li R, Li H, Tong J. Integrating scRNA-seq to explore novel macrophage infiltration-associated biomarkers for diagnosis of heart failure. BMC Cardiovasc Disord. 2023;23(1):560.
56. Mia MM, Cibi DM, Abdul Ghani SAB, Song W, Tee N, Ghosh S, Mao J, Olson EN, Singh MK. YAP/TAZ deficiency reprograms macrophage phenotype and improves infarct healing and cardiac function after myocardial infarction. PLoS Biol. 2020;18(12):e3000941.
57. Meng Q, Liu H, Liu J, Pang Y, Liu Q. Advances in immunotherapy modalities for atherosclerosis. Front Pharmacol. 2022;13:1079185.
58. Wang Z, Xu Y, Wang M, Ye J, Liu J, Jiang H, Ye D, Wan J. TRPA1 inhibition ameliorates pressure overload-induced cardiac hypertrophy and fibrosis in mice. EBioMedicine. 2018;36:54–62.
59. Zhuang L, Zong X, Yang Q, Fan Q, Tao R. Interleukin-34-NF-kappaB signaling aggravates myocardial ischemic/reperfusion injury by facilitating macrophage recruitment and polarization. EBioMedicine. 2023;95:104744.
60. Liu S, Wang T, Cheng Z, Liu J. N6-methyladenosine (m6A) RNA modification in the pathophysiology of heart failure: a narrative review. Cardiovasc Diagn Ther. 2022;12(6):908–25.
61. Wang T, Tian J, Jin Y. VCAM1 expression in the myocardium is associated with the risk of heart failure and immune cell infiltration in myocardium. Sci Rep. 2021;11(1):19488.
62. Dubey PK, Patil M, Singh S, Dubey S, Ahuja P, Verma SK, Krishnamurthy P. Increased m6A-RNA methylation and FTO suppression is associated with myocardial inflammation and dysfunction during endotoxemia in mice. Mol Cell Biochem. 2022;477(1):129–41.
63. Bajpai G, Bredemeyer A, Li W, Zaitsev K, Koenig AL, Lokshina I, Mohan J, Ivey B, Hsiao HM, Weinheimer C, et al. Tissue Resident CCR2- and CCR2 + Cardiac macrophages differentially orchestrate Monocyte Recruitment and Fate Specification following myocardial Injury. Circ Res. 2019;124(2):263–78.
64. Epelman S, Lavine KJ, Beaudin AE, Sojka DK, Carrero JA, Calderon B, Brija T, Gautier EL, Ivanov S, Satpathy AT, et al. Embryonic and adult-derived resident cardiac macrophages are maintained through distinct mechanisms at steady state and during inflammation. Immunity. 2014;40(1):91–104.
65. Zhang K, Wang Y, Chen S, Mao J, Jin Y, Ye H, Zhang Y, Liu X, Gong C, Cheng X, et al. TREM2(hi) resident macrophages protect the septic heart by maintaining cardiomyocyte homeostasis. Nat Metab. 2023;5(1):129–46.
66. Dick SA, Macklin JA, Nejat S, Momen A, Clemente-Casares X, Althagafi MG, Chen J, Kantores C, Hosseinzadeh S, Aronoff L, et al. Self-renewing resident cardiac macrophages limit adverse remodeling following myocardial infarction. Nat Immunol. 2019;20(1):29–39.
67. Jia D, Chen S, Bai P, Luo C, Liu J, Sun A, Ge J. Cardiac Resident macrophage-derived Legumain improves Cardiac Repair by promoting clearance and degradation of apoptotic cardiomyocytes after myocardial infarction. Circulation. 2022;145(20):1542–56.
68. Jordan E, Peterson L, Ai T, Asatryan B, Bronicki L, Brown E, Celeghin R, Edwards M, Fan J, Ingles J, et al. Evidence-based Assessment of genes in dilated cardiomyopathy. Circulation. 2021;144(1):7–19.
69. Wu Y, Jiang D, Zhang H, Yin F, Guo P, Zhang X, Bian C, Chen C, Li S, Yin Y, et al. N1-Methyladenosine (m1A) regulation Associated with the pathogenesis of abdominal aortic aneurysm through YTHDF3 modulating macrophage polarization. Front Cardiovasc Med. 2022;9:883155.
70. Tong J, Wang X, Liu Y, Ren X, Wang A, Chen Z, Yao J, Mao K, Liu T, Meng FL et al. Pooled CRISPR screening identifies m(6)a as a positive regulator of macrophage activation. Sci Adv. 2021;7(18).
71. Liu Y, Liu Z, Tang H, Shen Y, Gong Z, Xie N, Zhang X, Wang W, Kong W, Zhou Y, et al. The N(6)-methyladenosine (m(6)A)-forming enzyme METTL3 facilitates M1 macrophage polarization through the methylation of STAT1 mRNA. Am J Physiol Cell Physiol. 2019;317(4):C762–75.
72. Zheng Y, Li Y, Ran X, Wang D, Zheng X, Zhang M, Yu B, Sun Y, Wu J. Mettl14 mediates the inflammatory response of macrophages in atherosclerosis through the NF-kappaB/IL-6 signaling pathway. Cell Mol Life Sci. 2022;79(6):311.
73. Liu Y, Zhang S, Gao X, Ru Y, Gu X, Hu X. Research progress of N1-methyladenosine RNA modification in cancer. Cell Commun Signal. 2024;22(1):79.
74. Smoczynski J, Yared MJ, Meynier V, Barraud P, Tisne C. Advances in the Structural and Functional understanding of m(1)a RNA modification. Acc Chem Res. 2024;57(4):429–38.

Publisher's Note